CLINICAL GENETICS An International Journal of Genetics, Molecular and Personalized Medicine

Clin Genet 2015: 87: 576–581
Printed in Singapore. All rights reserved

CLINICAL GENETICS
doi: 10.1111/cge.12426

Short Report

Methylmalonic aciduria *cblB* type: characterization of two novel mutations and mitochondrial dysfunction studies

Brasil S., Richard E., Jorge-Finnigan A., Leal F., Merinero B., Banerjee R., Desviat L.R., Ugarte M., Pérez B. Methylmalonic aciduria *cblB* type: characterization of two novel mutations and mitochondrial dysfunction studies.
Clin Genet 2015: 87: 576–581. © John Wiley & Sons A/S. Published by John Wiley & Sons Ltd, 2014

Methylmalonic aciduria (MMA) *cblB* type is caused by mutations in the *MMAB* gene, which codes for the enzyme adenosine triphosphate (ATP): cobalamin adenosyltransferase (ATR). This study reports differences in the metabolic and disease outcomes of two pairs of siblings with MMA *cblB* type, respectively harbouring the novel changes p.His183Leu/p.Arg190dup (P1 and P2) and the previously described mutations p.Ile96Thr/p.Ser174fs (P3 and P4). Expression analysis showed p.His183Leu and p.Arg190dup to be destabilizing mutations. Both were associated with reduced ATR stability and a shorter half-life than wild-type ATR. Analysis of several parameters related to oxidative stress and mitochondrial function showed an increase in reactive oxygen species (ROS) content, a decrease in mitochondrial respiration and changes in mitochondria morphology and structure in patient-derived fibroblasts compared to control cells. The impairment in energy production and the presence of oxidative stress and fission of the mitochondrial reticulum suggested mitochondrial dysfunction in *cblB* patients' fibroblasts. The recovery of mitochondrial function should be a goal in efforts to improve the clinical outcome of MMA *cblB* type.

Conflict of interest

The authors declare that they have no conflict of interest.

S. Brasil[a,b,c,d], E. Richard[a,b,c], A. Jorge-Finnigan[a,e], F. Leal[a,b,c], B. Merinero[a,b,c], R. Banerjee[f], L.R. Desviat[a,b,c], M. Ugarte[a,b,c] and B. Pérez[a,b,c]

[a]Centro de Diagnóstico de Enfermedades Moleculares, Centro de Biología Molecular-SO UAM-CSIC, Universidad Autónoma de Madrid, Madrid, Spain, [b]Centro de Investigación Biomédica en Red de Enfermedades Raras (CIBERER), Madrid, Spain, [c]Instituto de Investigación Biomédica, IDIPaz, Madrid, Spain, [d]Metabolism & Genetics Group, Research Institute for Medicines and Pharmaceuticals Sciences (iMed.UL), Faculty of Pharmacy, University of Lisbon, Lisbon, Portugal, [e]Department of Biomedicine, University of Bergen, Bergen, Norway, and [f]Department of Biological Chemistry, University of Michigan Medical School, Ann Arbor, MI, USA

Key words: methylmalonic aciduria – mitochondrial function – *MMAB* gene – mutation

Corresponding author:
Dr Belén Pérez, Centro de Diagnóstico de Enfermedades Moleculares, Centro de Biología Molecular-SO UAM-CSIC, Universidad Autónoma Madrid, Campus de Cantoblanco, 28049 Madrid, Spain.
Tel.: +34 911964566;
fax: +34 911964420;
e-mail: bperez@cbm.csic.es

Received 7 February 2014, revised and accepted for publication 8 May 2014

ATP:cob(I)alamin adenosyltransferase (ATR, E.C.2.5.1.17) is involved in coenzyme B_{12} metabolism, converting reduced cob(I)alamin to adenosylcobalamin. The latter is the active cofactor of methylmalonyl-CoA mutase (MUT, EC 5.4.99.2), which catalyses the reversible rearrangement of methylmalonyl-CoA to succinyl-CoA during the catabolism of branched-chain amino acids, odd-chain fatty acids and cholesterol. Mutations in the human *MMAB* gene coding for ATR are responsible for methylmalonic aciduria (MMA) *cblB* type (OMIM #607568). Patients with MMA *cblB* type suffer either a severe, early-onset form of the

disease, with neonatal ketoacidosis, lethargy, failure to thrive and encephalopathy, or a milder late-onset form usually diagnosed during infancy that has a less serious neurological outcome (1).

To date, 32 different mutations have been identified in the *MMAB* gene in *cblB* patients (HGMD® Professional Release 2013.4). Several of these have been functionally analysed and their kinetic parameters determined in prokaryotic and eukaryotic expression systems. These studies have revealed the existence of mutants with reduced substrate and cofactor affinity (p.R191W) (2), and with negligible activity and presumed instability *in vivo* (p.R186W, p.R190H and p.E193K) (3), as well as destabilizing mutations that retain some residual activity (4).

Mitochondrial dysfunction is involved in a number of human genetic diseases, including inherited metabolic problems (5–7). In MMA, mitochondrial impairment occurs through the combination of the specific inhibition of mitochondrial enzymes, the inhibition of respiratory complexes, transport inhibition, the restriction of certain substrates for the tricarboxylic acid (TCA) cycle, and oxidative damage (8, 9). In fact, in MMA, the mitochondrial functional impairment observed in different organs and fibroblasts from patients, and in mouse models, has been proposed to be partly responsible for increased intracellular reactive oxygen species (ROS) levels leading to oxidative stress (7, 9–11). Genes involved in controlling oxidative stress might therefore act as phenotype modifiers, helping to explain the different disease presentations in patients with identical genotypes, as described in oxidative phosphorylation (OXPHOS) disorders (12).

The aim of the present study was to determine the pathogenic mechanisms of action of two new changes, c.548A> T and c.568_570dup, detected in a patient identified in an expanded newborn screening program. Mitochondrial function in cells from two pairs of *cblB* siblings harbouring either the new changes, or the previously described changes c.287T>C and c.584G A was also examined.

Materials and methods

The patients examined were two sets of siblings (P1 and P2; P3 and P4). P1 was identified by expanded newborn screening; a diagnosis of MMA was performed by gas chromatography-mass spectrometry (GC-MS) analysis of organic acids in urine. P2 was identified by the family genetic study and showed a slight increase in urine methylmalonic acid (Table 1). P3 and P4 have been previously described (4, 11). Control fibroblasts (GM09503, GM08680, GM5756, GM8429 and GM5381) were obtained from the NIGMS Human Genetic Cell Repository (Coriell Institute for Medical Research, NJ). The present study was approved by the Ethics Committees of the *Universidad Autónoma de Madrid*. Written permission to perform genetic studies was provided by the patients' parents.

Human ATR protein and p.H183L (c.548A>T) and p.R190dup (c.568_570dup) mutants were expressed in *Escherichia coli*; the purification, ATR specific activity

Table 1. Biochemical, clinical and genetic findings[a]

Patients	MMA levels at diagnosis (mmol/mol creat)	[^{14}C]-Propionate nmol/10 h/mg protein−/+ (fold)[b]	Paternal allele[c]	Maternal allele[c]	Onset	Outcome	Reference
P1	830	0.63/1.19 (2×)	c.548A>T p.His183Leu	c.568_570dup p.Arg190dup	NBS	Asymptomatic	This work
P2	58	1.06/2.59 (3×)	c.548A>T p.His183Leu	c.568_570dup p.Arg190dup	–	9 years asymptomatic Studied due to previous affected sibling	This work
P3	2507	0.26/1.01 (3.8×)	c.287T>C p. Ile96Thr	c.584G>A p.Ser174fs	Late onset	Died at 4 years of age	(4, 11)
P4	3022	0.28/0.66 (2.4×)	c.287T>C p. Ile96Thr	c.584G>A p. Ser174fs	–	7 years asymptomatic. Studied due to previous affected sibling	(4, 11)
Controls	1–13	1.90 ± 1.18/2.34 ± 1.61	–	–		–	

NBS, newborn screening; NV, normal value.

[a]P1 has been investigated several times under mild hypoproteic diet, carnitine supplementation, cobalamin injections or cyanocobalamin oral administration. Urine methylmalonic aciduria (MMA) has varied between 28 and 100 mmol/mol creat (NV: <15), methylcitrate has slightly increased, C3-carnitine 1–4.4 µmol/l (NV: 0.15–0.89) and amino acid levels were normal in plasma and urine. P2 has been investigated under normal protein intake and without cobalamin injections during 3 years. Urine MMA excretion varied between 53 and 92 mmol/mol creat (NV: <15). Amino acids in plasma and urine; plasma vitamin B12 and methylcitrate in urine were in the control range. Only mild increases of C3-carnitine were detected (1.07–2.24 µmol/l; NV: 0.15–0.89).

[b][^{14}C]-Propionate uptake (nmol/10 h/mg protein) without/with (−/+) hydroxocobalamin.

[c]Mutations according to NM_052845.3.

and K_M values were assayed as described (4). The stability of the wild-type and p.H183L and p.R190dup proteins was measured by incubation at 27°C or 37°C. Soluble supernatants were incubated at 27°C or 37 °C and aliquots were removed at different times for sodium dodecyl sulfate polyacrylamide gel electrophoresis (SDS-PAGE). Immunodetection was performed using anti-ATR antibody diluted 1:1000 (ProteinTech Group Inc., Chicago, IL). Mitochondria isolation from fibroblasts was performed using anti-TOM22 MicroBeads (Miltenyi Biotec, Bergisch Gladbach, Germany).

ROS assays were performed in fibroblasts from three controls (GM9503, GM8680 and GM5756) and from all patients, as described (11).

For bioenergetic analysis, control and patient-derived fibroblasts (5×10^4 each) were seeded per well in 24-well microplates and incubated with Dulbecco's modified Eagle's medium (DMEM) supplemented with glucose or galactose (4.5 g/l, DMEM-Glu or DMEM-Gal) overnight at 37°C. Cells were then washed with phosphate buffered saline (PBS); 700 µl of DMEM-Glu or DMEM-Gal without bicarbonate were added and the plates incubated at 37°C for 1 h. Modulating compounds such as oligomycin (OL, 6 µM), carbonyl cyanide 4-(trifluoromethoxy) phenyl-hydrazone (FCCP, 50 µM), rotenone (RO, 1 µM) and antimycin A (AT, 1 µM) were used to assess the bioenergetic profile. Oxygen consumption rate (OCR) was measured using a Seahorse XF24 Extracellular Flux Analyser (Seahorse Bioscience, Billerica, MA). The calibration plate for these compounds was prepared according to the manufacturer's protocol.

For mitochondrial morphology, 100,000 fibroblasts were seeded on a 10 mm glass coverslip and incubated with MEM at 37°C overnight. Cells were then incubated with 500 nM Mitotracker® Red CM-H2Ros probe (Life Technologies, Grand Island, NY) at 37°C for 40 min, and fixed in 10% formalin at room temperature for 20 min. Cells were washed with PBS and mounted facing downwards in mounting medium on a microscope slide. Images were taken using an Axiovert200 inverted microscope (Zeiss, Jena, Germany; magnification ×63) equipped with a DsRED filter.

For electron microscopy, fibroblasts were fixed for 1 h in the culture plates with 4% paraformaldehyde and 2% glutaraldehyde. Pellets were dehydrated and embedded in Epon resin.

Results

P1, classified as belonging to MMA *cblB* type by somatic cell complementation assay, is clinically asymptomatic and follows a disease management plan to avoid metabolic crises. His sibling, P2, is asymptomatic. Notably, P2-derived fibroblasts showed a [^{14}C]-propionate uptake incorporation close to normal, which decreased significantly when subjected to heat shock at 42°C (Fig. 1a). The levels of mitochondrial ATR protein have been assayed and only some traces of immunoreactive protein could be detected in P1 and P2 patients-derived fibroblasts (data not shown).

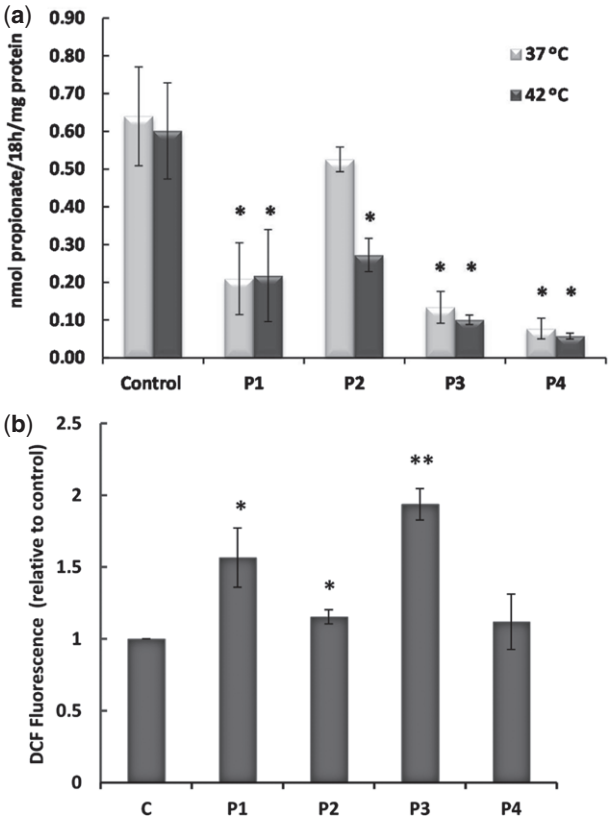

Fig. 1. [^{14}C]-Propionate incorporation and intracellular ROS content in control- and patient-derived fibroblasts. (**a**) [^{14}C]-Propionate incorporation was performed by incubation of dermal fibroblasts at 37°C or 42°C in the absence of hydroxocobalamin (OHCbl) to provide an indirect quantification of adenosyltransferase (ATR) activity. Results are the means ± SD of three independent experiments (*$p < 0.05$). (**b**) Intracellular ROS content of control and patients' fibroblasts. Cells were incubated with the H_2DCFDA fluorescence probe, and ROS levels assessed by flow cytometry. The x-axis represents patient cell lines and the y-axis the fluorescence levels. Control value was determined as the mean of data from the three control cell lines. Data are the mean ± SD of five independent experiments, each performed in triplicate. Data were analysed by analysis of variance (ANOVA; using SPSS software) with Bonferroni correction (*$p < 0.05$, **$p < 0.01$).

Genetic analysis revealed the presence of two novel mutations in exon 7 in P1 and P2; one exonic paternal change probably leading to a missense mutation p.H183L (c.548A>T), and one maternal small in-frame duplication, p.R190dup (c.568_570dup). Both changes were absent in the Exome Variant database (evs.gs.washington.edu). They were classified as 'probably damaging' by PolyPhen2 (genetics.bwh.harvard.edu/pph2) and SIFT (sift.jcvi.org/). No other changes or copy number variations were found after promoter sequencing and analysis using a customized high-resolution comparative genomic hybridization assay (Metaboloarray®, Agilent, SantaClara, CA) (13).

ATR activity was measured, and the K_M for the substrates, adenosine triphosphate (ATP) and hydroxocobalamin (OHCbl) were determined using *E. coli* cell lysates expressing wild-type or mutant proteins. An approximately 75-fold reduction in specific

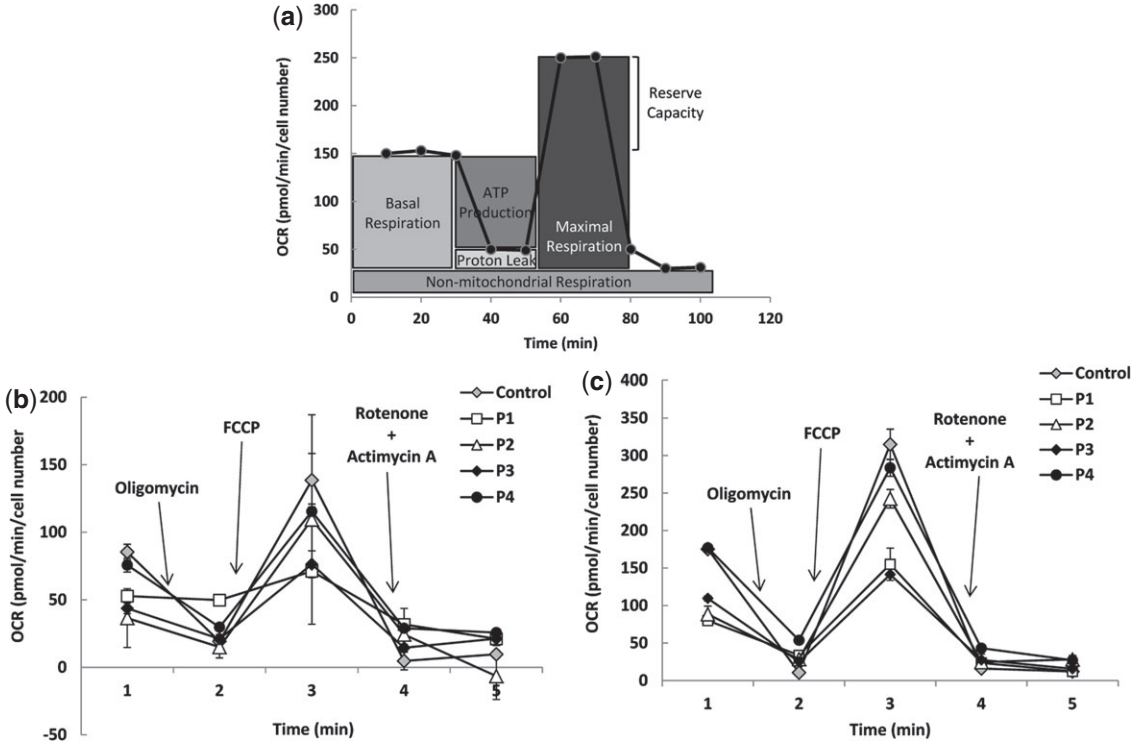

Fig. 2. Bioenergetic profile of control- and patient-derived fibroblasts. (**a**) The fundamental parameters of mitochondrial function: basal respiration, adenosine triphosphate (ATP) turnover, proton leak, and maximal respiration, or spare respiratory capacity. (**b**) and (**c**) Bioenergetic profile of patients' and controls' fibroblasts cultured in two different kinds of media. Cells were incubated with DMEM supplemented with glucose (**b**) or galactose (**c**) and the oxygen consumption rate (OCR) profile in each case after the addition of oligomycin, carbonyl cyanide 4-(trifluoromethoxy) phenyl-hydrazone (FCCP), rotenone and antimycin A was measured. Data are the mean ± SD of three independent experiments, each performed in triplicate. Further analysis to rescue the phenotype after MMAB complementary DNA (cDNA) correction will be performed in the near future.

activity was seen compared to the wild-type in the crude extract of bacteria expressing p.His183Leu. The purification yield was ∼100-fold higher for wild-type *vs* p.His183Leu. The kinetic data on purified ATR showed that the p.His183Leu possessed specific activities indistinguishable within experimental variation (0.21 ± 0.01 μmol/mg/min) than the wild type (0.23 ± 0.01 μmol/mg/min). The K_M^{ATP} (5.1 ± 1.4 μM) and K_M^{OHCbl} (0.71 ± 0.56 μM) values for this mutant were similar to those of wild type ($K_M^{ATP} = 6.2 \pm 1.3$ μM and $K_M^{OHCbl} = 1.7 \pm 0.4$ μM). The p.Arg190dup mutant did not show detectable activity in crude extracts and could not be purified.

The relative half-life of p.His183Leu mutant at 37°C was ∼50% that of wild-type (2.5 *vs* 5.4 h). At 27°C, however, p.His183Leu showed a marked increase in stability (7.6 *vs* 6.1). As expected, the p.Arg190dup was highly unstable and could not be examined under any conditions.

Flow cytometry showed a significant increase of ROS content in P1 cells and a moderate increase in P2 cells compared to control fibroblasts. P3 cells also showed a greater increase in ROS content than P4 cells (Fig. 1b).

For bioenergetic profile OL, FCCP, RO and AT were sequentially added to the cells and the fundamental parameters of mitochondrial function obtained are represented in Fig. 2a. O_2 consumption by fibroblasts revealed that cells grown in DMEM-Glu (Fig. 2b) or DMEM-Gal (Fig. 2c) had similar bioenergetic profiles. OCR was reduced in all patient-derived fibroblasts incubated in either medium, with a shift observed towards higher values in control and patient fibroblasts grown in DMEM-Gal; indeed, these reached control levels in P2 and P4. This shift is due to an increase in the aerobic production of ATP in the absence of glucose. The basal respiratory rates were markedly lower in P1-, P2- and P3-derived fibroblasts compared to controls. The maximum OCR after the injection of FCCP into DMEM-Glu was lower in patients' fibroblasts (Fig. 2b), and was doubled in all fibroblasts grown in DMEM-Gal (Fig. 2c). A reduction in OCR was observed after the addition of OL. The difference between basal OCR levels and post-OL addition represents the effect of ATP-linked respiration. In the DMEM-Glu medium, a fall in ATP-linked respiration was observed in all patient-derived fibroblasts compared to controls, especially in P1 (Fig. 2b). In DMEM-Gal, ATP-linked respiration was higher in all patient-derived fibroblasts, especially in P4 (Fig. 2c).

Marked fission of the mitochondrial reticulum was seen in all patient-derived fibroblasts, and mitochondria were seen to gather around the perinuclear area in P3 cells. Compared to controls, a significantly increased proportion of grain-like structures were seen in P1, P2 and P3 cells and to a lesser extent in P4 (Fig. 3a and b). In addition, *cblB* fibroblasts presented a reduced number of mitochondria and had a distinct mitochondria

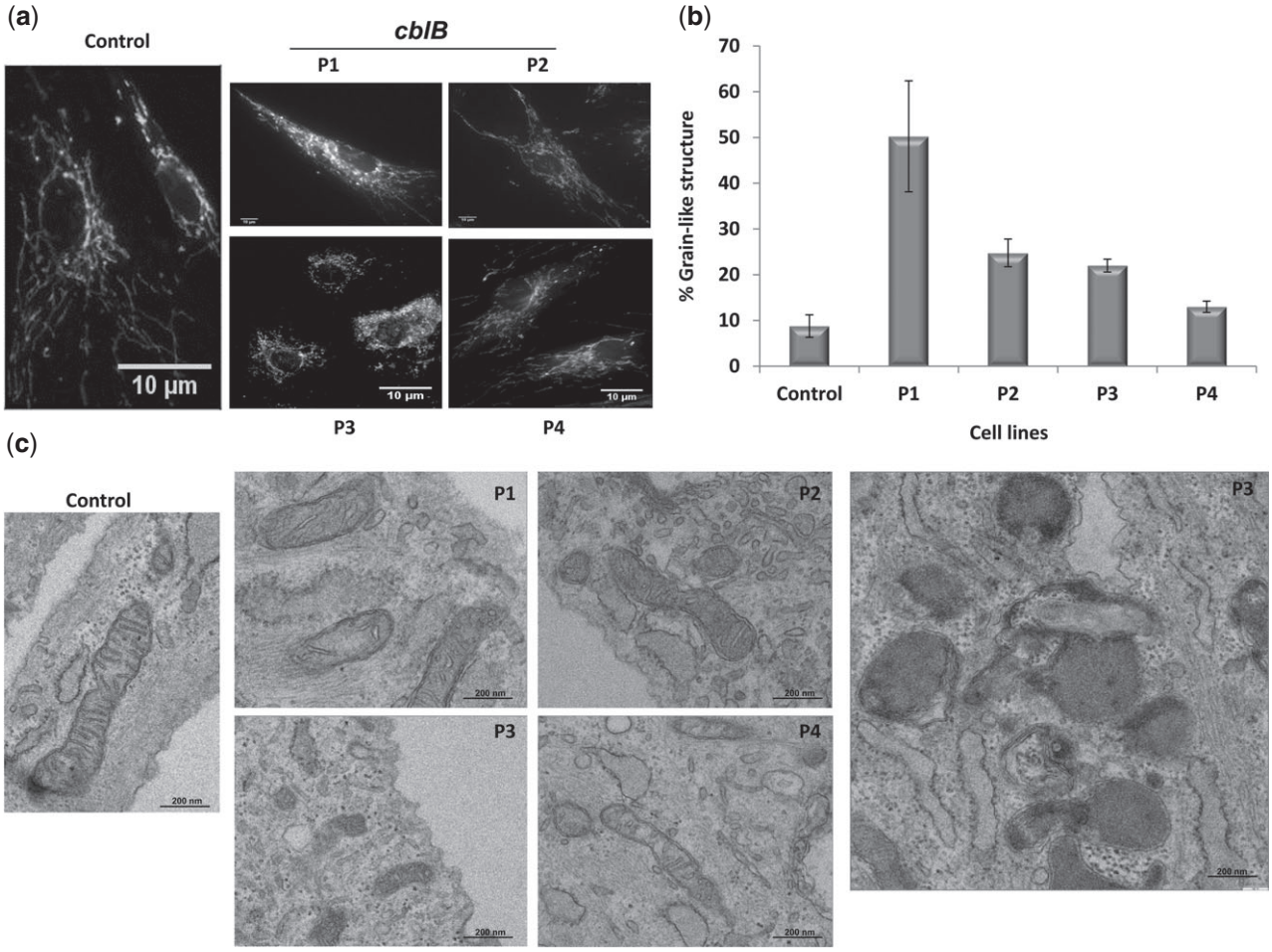

Fig. 3. Mitochondrial morphology and ultrastructure of control- and patient-derived fibroblasts. (**a**) Representative images of mitochondrial morphology of control and patients' fibroblasts (P1, P2, P3 and P4). Cells labelled with MitoTracker®Red CM-H2Ros revealed two distinct phenotypes: thread-like (control) and grain-like (P1, P2, P3 and P4), the latter associated with mitochondrial fission. (**b**) Quantification after MitoTracker®Red CM-H2Ros label of the mitochondrial phenotypes observed in three independent experiments (each bar represents a minimum of 40 images containing a minimum of 2–3 cells). The results represent the mean ± SD of three independent experiments. (**c**) Representative electron micrographs of control- and patient-derived fibroblasts. Healthy control mitochondria contained groups of parallel cristae, which often extended through the entire body of the organelle and presented a dense mitochondrial matrix. On the contrary, *cblB* mitochondria had a distinct morphology indicating changes in mitochondria structure. Bars: 200 nm.

morphology including a marked decrease in size, a striking lack of cristae and a rarefaction of matrix density compared to controls (Fig. 3c).

Discussion

The functional analysis data reported herein suggest that the patient-associated changes p.His183Leu and p.Arg190dup are destabilizing mutations. Both changes were associated with reduced ATR stability and half-life, as described for other *cblB* mutations such as p.Ile96Thr and p.Arg191Trp (4). p.Arg190dup is a severely destabilizing mutation with concomitant greatly reduced ATR activity; p.His183Leu has a milder effect. The results suggest that p.His183Leu might be a misfolding mutation with low residual activity in bacterial crude extract; the purified mutant enzyme exhibits a specific activity, K_M^{ATP} and K_M^{OHCbl} values that are within the wild-type range.

Other evidence suggest that p.His183Leu and p.Arg 190dup are folding mutations including the [^{14}C]-propionate incorporation results under basal and stress conditions. While P1 showed lower propionate uptake than the controls under basal conditions, P2 cells only showed a propionate pathway defect. The present results are consistent with the idea that protein instability under physiological stress is indicative of a high risk of metabolic decompensation during illness, especially when fever is present, as described (14). Differences in the propionate pathway in P1 and P2 cells are probably explained by changes in the expression of proteins involved in the protein quality control system.

In all patient-derived fibroblasts, ROS content, the bioenergetic profile and mitochondrial structure were markedly different compared to those of control cells. The mitochondrial reserve capacity of the patients' fibroblasts was reduced, a problem known to occur in short-chain acyl-CoA dehydrogenase disorder (SCAD)

in the presence of destabilizing mutations (15). Moreover, the present results reflect significant differences in clinical outcome between siblings with the same genotype; P2 and P4, who had better clinical outcomes than their respectively siblings P1 and P3, appeared to suffer less mitochondrial dysfunction.

Grain-like structures have been related to mitochondrial fission, a mechanism involved in the maintenance of mitochondrial function and the preservation of the mitochondrial genome, but also in pre-apoptotic events (16). These grain-like structures were observed in all four patient-derived fibroblasts. The marked structural modification we report in *cblB* mitochondria may be correlated with a decrease in the efficiency of oxygen reduction and ATP generation and an increase in ROS production. In addition, laminar bodies and autophagosomes engulfing mitochondria were observed in *cblB* cells suggesting that autophagy is characterized by a selective mitophagy. These promising results will be followed up with further studies.

The improvement of mitochondrial dysfunction has been proposed as a new therapeutic goal in several human disorders. Treatment of these pathologies is not straightforward, but would probably involve combinations of conventional and novel pharmacological treatments plus nutritional interventions, including the possible consumption of antioxidants to reduce the ROS content in specific tissues and organs (17).

Acknowledgments

We acknowledge the patients and their families for their collaboration. This work was funded by grants from the Fondo de Investigaciones Sanitarias (PI13/01239 to B. P.), MITOLAB (S2010/BMD-2402 to B. P.), the Spanish Ministerio de Economía y Competividad (SAF2010-15284 to E. R.) and the National Institutes of Health (DK45776 to R. B.). S. B. was supported by a grant from the Fundação para a Ciência e Tecnologia of Portugal (SFRH/BD/45753/2008). An institutional grant from the Fundación Ramón Areces to the Centro de Biología Molecular Severo Ochoa is gratefully acknowledged.

References

1. Fowler B, Leonard JV, Baumgartner MR. Causes of and diagnostic approach to methylmalonic acidurias. J Inherit Metab Dis 2008: 31: 350–360.
2. Lofgren M, Banerjee R. Loss of allostery and coenzyme B12 delivery by a pathogenic mutation in adenosyltransferase. Biochemistry 2011: 50: 5790–5798.
3. Zhang J, Dobson CM, Wu X et al. Impact of cblB mutations on the function of ATP:cob(I)alamin adenosyltransferase in disorders of vitamin B12 metabolism. Mol Genet Metab 2006: 87: 315–322.
4. Jorge-Finnigan A, Aguado C, Sanchez-Alcudia R et al. Functional and structural analysis of five mutations identified in methylmalonic aciduria cblB type. Hum Mutat 2010: 31: 1033–1042.
5. Richard E, Jorge-Finnigan A, Garcia-Villoria J et al. Genetic and cellular studies of oxidative stress in methylmalonic aciduria (MMA) cobalamin deficiency type C (cblC) with homocystinuria (MMACHC). Hum Mutat 2009: 30: 1558–1566.
6. Karbowski M, Neutzner A. Neurodegeneration as a consequence of failed mitochondrial maintenance. Acta Neuropathol 2012: 123: 157–171.
7. Wajner M, Goodman SI. Disruption of mitochondrial homeostasis in organic acidurias: insights from human and animal studies. J Bioenerg Biomembr 2011: 43: 31–38.
8. Melo DR, Kowaltowski AJ, Wajner M, Castilho RF. Mitochondrial energy metabolism in neurodegeneration associated with methylmalonic acidemia. J Bioenerg Biomembr 2011: 43: 39–46.
9. Chandler RJ, Zerfas PM, Shanske S et al. Mitochondrial dysfunction in mut methylmalonic acidemia. FASEB J 2009: 23: 1252–1261.
10. Richard E, Monteoliva L, Juarez S et al. Quantitative analysis of mitochondrial protein expression in methylmalonic acidemia by two-dimensional difference gel electrophoresis. J Proteome Res 2006: 5: 1602–1610.
11. Richard E, Alvarez-Barrientos A, Perez B, Desviat LR, Ugarte M. Methylmalonic acidaemia leads to increased production of reactive oxygen species and induction of apoptosis through the mitochondrial/caspase pathway. J Pathol 2007: 213: 453–461.
12. Moran M, Rivera H, Sanchez-Arago M et al. Mitochondrial bioenergetics and dynamics interplay in complex I-deficient fibroblasts. Biochim Biophys Acta 1802: 2010: 443–453.
13. Perez B, Gutierrez-Solana LG, Verdu A et al. Clinical, biochemical, and molecular studies in pyridoxine-dependent epilepsy. Antisense therapy as possible new therapeutic option. Epilepsia 2013: 54: 239–248.
14. Maier EM, Gersting SW, Kemter KF et al. Protein misfolding is the molecular mechanism underlying MCADD identified in newborn screening. Hum Mol Genet 2009: 18: 1612–1623.
15. Schmidt SP, Corydon TJ, Pedersen CB, Bross P, Gregersen N. Misfolding of short-chain acyl-CoA dehydrogenase leads to mitochondrial fission and oxidative stress. Mol Genet Metab 2010: 100: 155–162.
16. Suen DF, Norris KL, Youle RJ. Mitochondrial dynamics and apoptosis. Genes Dev 2008: 22: 1577–1590.
17. Breuer ME, Willems PH, Russel FG, Koopman WJ, Smeitink JA. Modeling mitochondrial dysfunctions in the brain: from mice to men. J Inherit Metab Dis 2012: 35: 193–210.